Materials Science Forum Vols. 495-497 (2005) pp. 1529-1534
online at http://www.scientific.net

Online available since 2005/09/15

Simulation of earing during deep drawing of bcc steel by use of a texture component crystal plasticity finite element method

D. Raabe[1,a], F. Roters[1,b] and Y. Wang[2,c]

[1]Max-Planck-Institut für Eisenforschung, Max-Planck-Str. 1, 40237 Düsseldorf, Germany

[2]Department of Metallurgical Engineering, University of Missouri-Rolla, MO 65409-0340, USA

[a]raabe@mpie.de, [b]roters@mpie.de, [c]yanwenw@umr.edu

Keywords: crystal plasticity, FEM, plastic deformation, anisotropy, modeling, earing, body-centered-cubic, sheet forming, springback, deep drawing.

Abstract. We present a numerical study on the influence of crystallographic texture on the earing behavior of a low carbon steel during cup drawing. The simulations are conducted by using the texture component crystal plasticity finite element method which accounts for the full elastic-plastic anisotropy of the material and for the explicit incorporation of texture including texture update. Several important texture components that typically occur in commercial steel sheets were selected for the study. By assigning different spherical scatter widths to them the resulting ear profiles were calculated under consideration of texture evolution. The study reveals that 8, 6, or 4 ears can evolve during cup drawing depending on the starting texture. An increasing number of ears reduces the absolute ear height. The effect of the orientation scatter width (texture sharpness) on the sharpness of the ear profiles was also studied. It was observed that an increase in the orientation scatter of certain texture components entails a drop in ear sharpness while for others the effect is opposite.

Introduction

Shape anisotropy of drawn parts may occur in the form of earing. It is a phenomenon which is associated with the texture and the resulting elastic-plastic anisotropy of metals [1-16]. Sheet steels usually have pronounced textures which they inherit from the preceding processing steps such as hot rolling, cold rolling, and heat treatment [17-23].

Various concepts exist to introduce texture-related sheet anisotropy into finite element models for sheet forming. The material anisotropy existing before sheet deformation can be incorporated either through an anisotropic yield surface function [e.g. 24-28] or directly via the use of crystal plasticity finite element models. The crystal plasticity finite element models are a direct implementation of crystallographic slip kinematics into finite element models. It was first suggested by Peirce, Needlemann, and Asaro [29-32]. Based on their work an implicit time-integration scheme was developed by Kalidindi et al. [33] and implemented in commercial finite element software in the form of a user-defined subroutine. Crystal plasticity finite element models provide a direct means for updating the material state via integration of the evolution equations for the crystal lattice orientation and the critical resolved shear stress. The deformation behavior of the grains is at each integration point determined by a crystal plasticity model, which accounts for plastic deformation by crystallographic slip and for the rotation of the crystal lattice during deformation. Pioneering related studies along these lines have been published by Mathur and Dawson [34], Smelser and Becker [35], and Beaudoin et al. [36]. Crystal plasticity finite element models represent elegant tools for detailed simulation studies of texture evolution and forming ansiotropy under realistic boundary conditions. Each integration point can represent one orientation or a set of grain orientations when combined with a homogenization model. Although the latter case (mapping of a representative texture on one integration point) is principally feasible, it entails long calculation times, turning the method less practicable for industry-scale applications. For rendering the crystal plasticity finite element models more flexible with respect to the treatment of large polycrystalline entities Raabe

and Roters recently introduced a texture component crystal plasticity finite element model [37,38]. The basic idea of this method consists in using a more effective way of describing the texture of macroscopic samples at each integration point, turning the method into a texture component crystal plasticity finite element method. Details on this approach are given in [37,38].
Only few systematic simulation studies were published on earing in body-centered-cubic steels. For instance, Bacroix and Gilormini [3] presented a detailed work on earing in polycrystalline materials by use of finite-element simulations. They used a texture-adjusted fourth-order strain-rate potential and its associated normality rule. The coefficients of the potential function were directly obtained from the texture coefficients. They applied the method successfully to a mild steel. The approach was capable of reproducing six ears for certain textures. Li et al. [39] predicted the earing behavior of cup drawn IF (interstitial free) steel sheets by use of a texture-based plastic potential formulation. The group of Nakamachi et al. [40,41] used an elastic-viscoplastic finite element method to simulate the six and four ears of drawn cups of body centered cubic polycrystals. In order to achieve this goal they used a large number of integration points in conjunction with a crystal plasticity finite element formulation. Each rotation matrix mapped at an integration points was assumed to represent one grain. The crystallites could hence rotate individually upon mechanical loading. The sheet metal forming simulations of Nakamachi et al. [40,41] were not only used to predict the earing behavior but also to assess texture effects on strain localization and failure. They authors reported that {111}<uvw> orientations (γ-fiber texture) are favorable while the {hkl}<001> texture components where less favorable for sheet formability of steels.
These studies provide excellent insight into the relationship between the initial crystallographic texture of steel sheets before cup drawing and the ear profiles after deformation. The present study aims at pushing this effort a step further by, first, rigorously incorporating texture update into the simulations according to the crystal plasticity scheme, second, by a systematic variation of the relevant texture components typically occurring in body-centered-cubic steels [22,23], and third, by systematically varying the orientational scatter width of those texture components. The simulations are conducted by using the texture component crystal plasticity finite element model. After an introduction to this method and to the model set-up we simulate the individual ear profiles resulting from some typical texture components of body-centered-cubic polycrystals. Subsequently, we discuss the effects of these texture components on the observed ear profiles and also the effects of changes in the scatter width of these textures on the ear profile.

Simulation Details

The finite element calculations were conducted by using MSC/Marc in conjunction with the user defined material subroutine HYPELA2 [42]. An implicit crystal plasticity procedure developed by Kalidindi et al. [33,43,44] was implemented and used for the time integration of the constitutive equations. Hardening of the ferritic low carbon body-centered-cubic steel was described in terms of a set of adjustable parameters, i.e. $\dot{\gamma}_0 = 0.001$ s^{-1} was used as reference value for the slip rate. The strain rate sensitivity m was taken as 0.05. As hardening matrix parameters we used $q^{\alpha\beta} = 1.0$ for coplanar slip systems and $q^{\alpha\beta} = 1.4$ for non-coplanar systems. The components of the elasticity tensor were taken as $C_{11} = 230.1$ GPa, $C_{12} = 134.6$ GPa, and $C_{44} = 116.6$ GPa. The values of the slip system hardening parameters h_0, a, and s_s, and the initial value of the slip resistance s_0 were taken to be h_0=180 MPa, s_s=148 MPa, a=2.25, and s_0=16 MPa. The potential slip system families are the 12 $\{111\}<111>$ and the 12 $\{112\}<111>$ systems. Fig. 1a shows the tool geometry. Due to the sample symmetry, only a quarter of the blank was modeled. Fig. 1b shows the mesh configuration of the specimen. The Coulomb friction coefficient was assumed to be μ=0.1 between the punch and the blank.

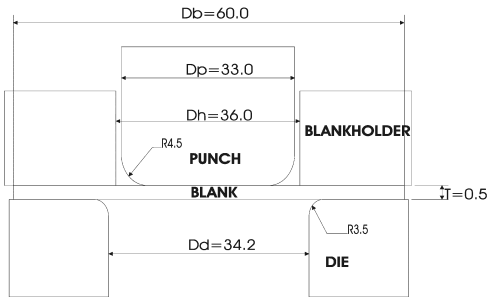

(a) Geometry of the tools.

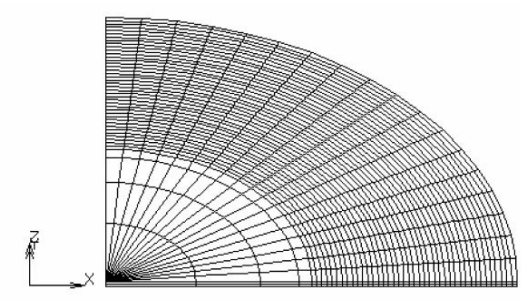

(b) mesh configuration.

Figure 1
(a) Finite element model showing the geometry of the tools in units of mm.
(b) Mesh configuration.

The texture components which typically occur with notable volume fractions in rolled and subsequently heat treated body centered cubic steel sheets [[22],[23],[45],[46]] are the {001}<110> (φ_1=0°, ϕ=0°, φ_2=45°), the (111)[1$\bar{1}$0] (φ_1=0°, ϕ=54.7°, φ_2=45°), and the (111)[11$\bar{2}$] component (φ_1=90°, ϕ=54.7°, φ_2=45°). While the {111}<uvw> texture components are the two most relevant orientations emerging during primary recrystallization the (001)[110] component is inherited from rolling owing to pronounced recovery [45,46]. Another important texture component often resulting from recrystallization is the φ_1=15°, ϕ=45°, φ_2=50° (≈(557)[58$\underline{3}$]) orientation which is about 10° off the {111}<uvw> fiber [22,23] (all Euler triples are given in Bunge notation [47].)
The texture component crystal plasticity finite element simulations in this study are conducted by using combinations of the texture components given above (with 7° and with 15° full width at half maximum) with a random background component. The incorporation of the random portion of the starting texture in the form of a pseudo-component may be important [16,38] because random *starting* textures do not *remain* random during forming. As any other orientation, randomly distributed orientations may gradually reorient and enhance anisotropy as a result of texture evolution. Although the contribution of the random pseudo-component is of course an isotropic one in the *beginning* of deformation it may evolve into an anisotropic one *during* deformation.
The random background texture component is in principle assigned to the integration points in the same way as the regular ideal texture components. This means that in the current study each integration point is described by one rotation matrix which is selected randomly from the set of spherical orientation component functions (typical texture components) and a second rotation matrix which is generated as a random orientation. Like the prescribed ideal texture components, the random texture component does cease to exist as a *component* in the further simulation procedure [37]. This is due to the fact that during the subsequent crystal plasticity finite element simulation each individual pair of orientations, originally pertaining to one of the texture components and to the random component, can undergo an *individual* orientation change as in the conventional crystal plasticity methods [30-33].
Owing to the orthorhombic sample symmetry each of the single orientations has in the starting texture to be balanced by three additional symmetrically equivalent orientations in order to correctly reproduce the response of the material in the calculations. Consequently, each of the symmetrical variants was assigned one quarter of the volume of the original component, i.e. 20vol.% of the total volume at one integration point. The remaining 20 vol.% is occupied by a random component. This initial symmetry operation is required since the starting data which are typically taken from x-ray data do not allow one to differentiate between the different symmetrical variants of a texture component owing to Friedel's law and to the symmetry group of the sample coordinate system.

Results and discussion

Fig. 2 shows the simulated ear profiles for the four individual texture components together with the random component for different scatter widths. Cup drawing of the two {111}<uvw> texture components (φ_1=0°, ϕ=54.7°, φ_2=45° and φ_1=90°, ϕ=54.7°, φ_2=45°, respectively) leads in either case to a 6 ear profile. This type of shape is in accordance with earlier studies. It can be explained in terms of the corresponding symmetry of the Schmid tensors of the {111}<uvw> texture components. While a specific {111}<uvw> orientation has a 3-fold symmetry at the beginning of loading the addition of the other 3 symmetrical equivalent orientations results in an altogether 6-fold symmetry. The fact that the 6 ears do not reach the same height, as predicted by homogenization theory, may be attributed to the effect of texture evolution. This observation suggests that both, the incorporation of a random background component and the use of a crystal plasticity method allowing for texture update, are necessary ingredients in such simulations.

The course of the ear profiles (for both scatter widths) of the $(111)[1\bar{1}0]$ component (φ_1=0°, ϕ=54.7°, φ_2=45°) shows a mirror symmetrical shape relative to 45° to those of the $(111)[11\bar{2}]$ component (φ_1=90°, ϕ=54.7°, φ_2=45°), Figs.2a,b. This symmetry can be explained in terms of some simple considerations about those <111> slip directions which predominantly determine the deformation of {111}<uvw> texture components in body centered steel sheets: The two texture components $(111)[1\bar{1}0]$ and $(111)[11\bar{2}]$ have a 30° rotation relationship among each other when rotated about their common [111] normal direction. Each of the two texture components has three dominant active slip directions. The initial symmetry operations explained above, which add to each orientation at an integration point 3 symmetrical equivalents (in the case of orthorhombic sample symmetry), contributes three more dominant active slip directions to each Gauss point. The resulting configuration for the two {111}<uvw> texture components then reveals a 45° symmetry relationship. This symmetry effect induced by the main <111> directions is visible in Figs.2a,b.

In the 6 ear profiles of the two {111}<uvw> texture components not all ears have the same height, i.e. two sets of three (symmetrically similar) ears differ from each other both in terms of height and shape. Fig.2b reveals that this effect is smoothened when the scatter width (full width at half maximum) of the initial texture components is increased from 7° (Fig.2a) to 15° (Fig.2b). The texture component φ_1=15°, ϕ=45°, φ_2=50° leads to 8 ears . Fig.2a shows that two sets of ears exist with different height and shape. The rotated cube component, φ_1=0°, ϕ=0°, φ_2=45°, (001)[110], reveals only 4 huge ears along the rim of the drawn cup. The presented ear profiles of the four individual texture components suggest that they essentially reproduce the symmetry of the crystallography of the center orientation relative to the sheet and forming symmetry.

According to the rim shapes characteristic differences occur in the ear height for the various starting textures. The φ_1=0°, ϕ=0°, φ_2=45° component shows a maximum variation in the ear height along the cup rim. This means that this component is detrimental with respect to isotropy. Owing to its impact on the overall shape and its 4-fold symmetry its effect on anisotropy cannot be easily compensated. Such compensation, which is for instance exploited in the field of aluminum forming [16], would require texture components with a shape anisotropy which is inverse to that of the φ_1=0°, ϕ=0°, φ_2=45° component. However, such orientations do not exist in typcial textures of steel sheets [18-23]. The conclusion from that is that the φ_1=0°, ϕ=0°, φ_2=45° texture component must be avoided in sheet steels which are subject to subsequent cup drawing operations.

The ear profile generated by the φ_1=0°, ϕ=54.7°, φ_2=45° and φ_1=90°, ϕ=54.7°, φ_2=45° texture components is much smoother when compared to that of the 45° rotated cube orientation. Furthermore, the occurrence of the two texture components with the same volume fraction together in one sheet leads to a perfect isotropic shape owing to their 30° <111> rotational or respectively 45° mirror equivalence, i.e. the planar anisotropy would be zero for such a case.

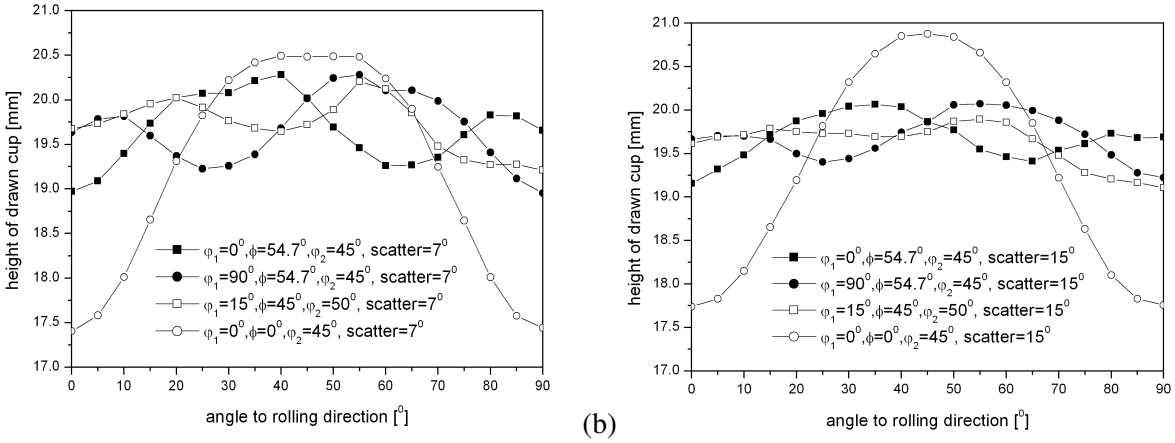

(a) (b)

Figure 2. Ear profiles of texture components with (a) scatter width 7^0 and (b) scatter width 15^0.

Conclusions

We used a texture component crystal plasticity finite element method to investigate the effect of texture on the earing behavior in body-centered-cubic steel sheets. We observed that the ear profiles depend strongly on the respective texture component: The two {111}<uvw> texture components (φ_1=0°, ϕ=54.7°, φ_2=45° and φ_1=90°, ϕ=54.7°, φ_2=45°) lead to 6 ears. The texture component φ_1=15°, ϕ=45°, φ_2=50° leads to 8 ears . The presence of the rotated cube component, φ_1=0°, ϕ=0°, φ_2=45°, leads to 4 huge ears. An increase in the number of ears entails a drop in the ear height. An increase in the orientation scatter of the texture component before deformation does not generally lead to a drop in the resulting shape anisotropy. Owing to its large in-plane anisotropy the rotated cube component should be avoided as a main texture component in body-centered-cubic steel sheets. The incorporation of a random texture component prior to mechanical loading is useful in order to account for texture evolution effects during forming. However, the current data and their comparison to earing predictions stemming from homogenization simulations suggests that the incorporation of a random texture component can be regarded as a second order effect. The texture component finite element method can be used as an engineering numerical laboratory which helps the user to decide which forming situations require the direct incorporation of texture including texture update and which do not. Also, it can be used to derive phenomenological constitutive data as input parameters for instance for yield surface simulations.

Acknowledgements

The authors are grateful to the Deutsche Forschungsgemeinschaft DFG (German Research Foundation) which is funding this study within the Schwerpunktprogramm 1138 (Modellierung von Größeneinflüssen bei Fertigungsprozessen).

References

[1] Van Houtte P, Mols K, Van Bael B, Aernoudt E, Textures and Microstructures 1989, 11:23.
[2] Hosford W F, The Mechan. Crystals and Textured Polycrystals, Oxford University Press 1993.
[3] Bacroix B, Gilormini P, Model. Simul. Mater. Sci. Eng. 1995, 3:1.
[4] Balasubramanian S, Anand L, Computational Mechanics 1996, 17:209.

[5] Hosford W F, Textures and Microstructures 1996, 26:479.
[6] Kocks U F, Tóme C N, Wenk H R, Texture and Anisotropy - Preferred Orientations in Polycrystals and Their Effect on Material Properties, Cambridge University Press 1998.
[7] Zhou Y, Jonas J J, Savoie J, Makinde A, MacEwen S R, Intern. J. Plasticity 1998, 14:117.
[8] Hu, J G, Jonas J J, Ishikawa T, Mater. Sc. Engin. A 1998, 256:51.
[9] Aretz H, Luce R, Wolske M, Kopp R, Goerdeler M, Marx V, Pomana G, Gottstein G, Model. Simul. Mater. Sci. Eng. 2000, 8:881.
[10] Peeters B, Hoferlin E, Van Houtte P, Aernoudt E, Intern. J. Plasticity 2001, 17:819.
[11] Becker R, Smelser R E, Panchanadeeswaran S, Modelling Simul Mater Sci Eng 1993,1:203.
[12] Beaudoin A J, Dawson P R, Mathur K K, Kocks U K, Korzekwa D A. Comput Methods Appl Mech Engrg 1994,117:49.
[13] Engler O, Kalz S, Mater. Sc. Engin. A 2004, 373:350.
[14] Chung Y H, Cho K K, Han J H, Shin M C, Scripta Mater. 2000, 43:759.
[15] Savoie J, Zhou Y, Jonas J J, MacEwen S R, 1996 Acta Mater., 44:587.
[16] Zhao Z, Mao W, Roters F, Raabe D: Acta Mater. 2004, 52:1003.
[17] Wassermann G, Grewen J, Texturen metall. Werkstoffe, Springer-Verlag, Germany 1969.
[18] Mishra S, Därmann C, Lücke K, Acta Met. 1984, 32:2185.
[19] Hutchinson W B, Int. Mat. Rev. 1984, 29:25.
[20] von Schlippenbach U, Emren F, Lücke K, Acta Metall. 1986, 34:1289.
[21] Ray R, Jonas J, Mat. Rev. 1990, 35:1.
[22] Hölscher M, Raabe D, Lücke K, Steel Research 1991, 62:567.
[23] Raabe D, Lücke K, Mater. Sc. Techn. 1993, 9:302.
[24] Hill R. Proc Royal Soc London 1948,A193:281.
[25] Hill R. Math Proc Cambridge Philos Soc 1949,85:179.
[26] Hosford W F, Seventh N, American Metalworking Res. Conf. Proc, 1979:191.
[27] Barlat F, Mater. Sc. Engin. 1987,91:55.
[28] Barlat F, Lian J., Int. Intern. J. Plasticity 1989,5:51.
[29] Pierce D, Asaro R J, Needleman A, Acta Metall. 1982, 30:1087.
[30] Asaro R J, Adv. appl. Mech. 1983, 23:1.
[31] Pierce D, Asaro R J, Needleman A, Acta Metall. 1983, 31:1951.
[32] Needleman A, Asaro R J, Acta Metall. 1985, 33:923.
[33] Kalidindi S R, Bronkhorst C A, Anand L, J. Mech. Phys. Solids 1992, 40: 537.
[34] Mathur K K, Dawson P R, Intern. J. Plasticity 1989, 5:67.
[35] Smelser R E, Becker R. ABAQUS User's Group Conf. Proc., Oxford 1999:457.
[36] Beaudoin A J, Dawson P R, Mathur K K, Kocks U F, Korzekwa D A. Comp Meth Appl Mech Eng 1994, 117:49.
[37] Raabe D, Roters F, Intern. J. Plasticity 2004, 20:339.
[38] Raabe D, Zhao Z, Roters F, Scripta Mater. 2004, 50:1085.
[39] Li S, Hoferlin E, Van Bael A, Van Houtte P, Adv. Engin. Mater. 2001, 3:990.
[40] Nakamachi E, Xie C L, Harimoto M, Intern. J. Mechan. Sc. 2001,43:631.
[41] Xie C L, Nakamachi E, Materials and Design 2002, 23:59.
[42] MSC. Marc user's manual, Vol.D, MSC Software Corporation, 2001.
[43] Raabe D, Sachtleber M, Zhao Z, Roters F, Zaefferer S, Acta Mater. 2001, 49:3433.
[44] Wang Y, Raabe D, Klüber C, Roters F, Acta Mater. 2004, 52:2229.
[45] Raabe D, Steel Research 1995, 66:222.
[46] Raabe D, Scripta metall. 1995, 33:735.
[47] Bunge H J, 1982 Texture analysis in materials science. Butterworths, London, England.